Cell Reports
Report

Grk5l Controls Heart Development by Limiting mTOR Signaling during Symmetry Breaking

Martin D. Burkhalter,[1] Gregory B. Fralish,[2] Richard T. Premont,[3] Marc G. Caron,[2,3,4] and Melanie Philipp[5,*]
[1]Leibniz Institute for Age Research, Fritz Lippmann Institute, 07745 Jena, Germany
[2]Department of Cell Biology, Duke University Medical Center, Durham, NC 27710, USA
[3]Department of Medicine, Duke University Medical Center, Durham, NC 27710, USA
[4]Department of Neurobiology, Duke University Medical Center, Durham, NC 27710, USA
[5]Department of Biochemistry and Molecular Biology, Ulm University, 89081 Ulm, Germany
*Correspondence: melanie.philipp@uni-ulm.de
http://dx.doi.org/10.1016/j.celrep.2013.07.036

SUMMARY

The correct asymmetric placement of inner organs is termed situs solitus and is determined early during development. Failure in symmetry breaking results in conditions ranging from randomized organ arrangement to a complete mirror image, often accompanied by severe congenital heart defects (CHDs). We found that the zebrafish homolog of mammalian G protein-coupled receptor kinase 5 (GRK5) employs noncanonical, receptor-independent functions to secure symmetry breaking. Knockdown of GRK5's closest homolog in zebrafish embryos, Grk5l, is sufficient to randomize cardiac looping and left-right asymmetry. Mechanistically, we found that loss of GRK5 increases mammalian target of rapamycin complex 1 (mTORC1) activity. This causes elongation of motile cilia in the organ of laterality, a consequence that is known to be sufficient to trigger aberrant organ arrangement. By fine-tuning mTORC1, GRK5 thus serves an unanticipated function during early development, besides its well-characterized role in the adult heart. These findings could implicate GRK5 as a susceptibility allele for certain cases of CHD.

INTRODUCTION

Congenital heart defects (CHDs) are frequently occurring developmental malformations that constitute a high risk for infant mortality (Pierpont et al., 2007). They are characterized by abnormal development of the heart and its connected structures. Importantly, heart development is precisely controlled spatially as well as temporally. It starts long before the actual heart tube or its progenitor cells become evident. In particular, the future heart's shape and placement relative to the other internal organs is determined by early left-right (LR) symmetry breaking in vertebrates (Ramsdell, 2005). At the cellular level, the most important structure for asymmetry is the temporal organ of laterality, which is a cup-like structure at the distal end of the notochord. Motile cilia within the temporal organ of laterality induce flow by a coordinated movement that triggers the expression of genes only on the left side of the body and thus internal asymmetry along the body axis (Essner et al., 2002; Okada et al., 2005; Oteíza et al., 2008). Not surprisingly, disturbances in the formation or function of the temporal organ of laterality interfere with proper heart development. This is reflected by the fact that CHDs are very common in individuals with irregular asymmetry establishment (Sutherland and Ware, 2009). This condition, in which internal organs appear to find their placement randomly, is known as isomerism, situs ambiguous, or heterotaxy. The seriousness of the condition varies widely. Some patients experience complete rearrangement of internal organs, such as in left or right isomerism, whereas in other patients (e.g., those with dextrocardia) the heart appears to be the only affected structure.

The molecular causes underlying ciliary diseases and as such situs anomalies have been the focus of many studies in the past decade. Many signaling cascades were found to be of importance, including basic morphogens such as Sonic hedgehog (Shh) and Bone morphogenetic protein 4 (Bmp4) (Schilling et al., 1999). In addition to these, the mammalian target of rapamycin (mTOR) pathway has emerged as a key pathway in ciliary physiology. Interestingly, mTOR activity appears to be controlled through bending of cilia. In kidney cells, loss of cilia or the movement thereof resulted in unrestricted mTOR signaling and cell growth (Boehlke et al., 2010). mTOR signaling has thus been implicated in the development of polycystic kidney disease (PKD) (Zullo et al., 2010), which belongs to the family of cilia-based diseases. In zebrafish, mTOR signaling was linked to symmetry breaking, and deregulated mTOR activity within the organ of laterality or during the stages when this organ is functional was shown to randomize lateralization (DiBella et al., 2009; Yuan et al., 2012).

G protein-coupled receptor kinase 5 (GRK5) is one of seven kinases in vertebrates that were named for their ability to terminate GPCR signal transduction (Premont and Gainetdinov, 2007). It is highly abundant in the heart, with the effect that GRK5 is a major regulator of cardiac GPCRs and thus has a vital influence on heart physiology (Chen et al., 2001; Eckhart et al., 2000; Liggett et al., 2008; Martini et al., 2008; Rockman et al., 1996). Recent studies revealed that GRK5 modulates signal transduction also from non-GPCR receptors and even nonreceptor proteins (Huang et al., 2011b). Together with its action on adrenoceptors (Chen et al., 2001; Rockman et al., 1996), it is capable of significantly altering cardiac physiology by interacting with molecules such as nuclear factor kappa B (NFκB) and histone deacetylases (Martini et al., 2008; Sorriento et al., 2010). These just recently discovered functions are also promoted by GRK5's ability to act not only close to the cell membrane but also in other subcellular localizations, such as the nucleus (Gold et al., 2012; Michal et al., 2012).

Interestingly, GRK5 is already expressed in the developing heart (Premont et al., 1999). We thus hypothesized that besides controlling proper heart physiology in the adult organism, GRK5 may play an additional, previously unreported role in heart formation during early development.

RESULTS AND DISCUSSION

GRK5 Facilitates Cardiac Looping

To investigate a potential role of GRK5 in the developing heart, we used zebrafish as a model because of its advantages for developmental studies. We applied a commonly used knockdown (KD) approach to generate GRK5 loss-of-function zebrafish embryos. Zebrafish have two genes located on two different chromosomes with homology to human GRK5. These homologs share little nucleotide sequence homology with each other. Multiple protein alignment analyses demonstrated that zebrafish Grk5l, encoded on chromosome 8, is a closer homolog to human GRK5 than is zebrafish Grk5 on chromosome 10 (Figures S1A and S1B). Thus, we designed a translation-blocking antisense morpholino (MO) targeting the 5′ UTR of Grk5l (Grk5l MO), as well as a five-base mismatch control MO (CTRL MO). To confirm that the translation-blocking MO targeting *grk5l* sufficiently depletes Grk5l, we coinjected capped messenger RNA (mRNA) encoding for a Grk5l-GFP fusion protein, which was preceded by parts of *grk5l*'s 5′ UTR. Embryos injected with Grk5l MO failed to produce GFP fluorescence (Figures 1A–A″). Moreover, KD efficiency was verified by western blot (Figure S1C) and an MO binding assay (Figure S1D). Importantly, the 5′ UTRs of both *grk5* variants in zebrafish are not conserved and MOs targeting *grk5l* are not predicted to bind to the UTR of *grk5*. We also did not find a feedback loop altering mRNA levels of *grk5* upon KD of Grk5l (Figure S1E), suggesting that any phenotype observed was likely due to specific KD of Grk5l.

MO-mediated KD of Grk5l initially resulted in viable embryos that were morphologically very similar to noninjected (NI) wild-type (WT) embryos or embryos injected with the CTRL MO (Figures 1B–B″). After KD of Grk5l, we allowed the embryos to develop further and observed that Grk5l KD induced pericardiac edema and cardiac dilatation (Figures 1C and 1D). Two additional MOs targeting Grk5l either upstream of the first MO in the 5′ UTR or downstream around the start codon validated this cardiac phenotype (Figures 1D and S1F). We then examined Grk5l expression in the heart and observed *grk5l* transcripts in cardiac tissue at 48 hr postfertilization (hpf; Figure 1E). Furthermore, depletion of Grk5l also affected the expression of genes in the heart, which were shown to be important for valve seeding (Figures 1F–1K'). Chamber formation occurred regularly (Figure 1L–1M′). Importantly, however, the hearts of Grk5l KD embryos injected with any of the three MOs either failed to loop or showed an inverse loop in roughly half of the embryos (Figures 1N and 1O), which might be attributed to failure in establishing LR asymmetry. KD of the single zebrafish homolog of GRK2 and GRK3, Grk2/3, displayed regular D-loops (Figure 1O). Interestingly, loss of the other Grk5 in zebrafish also resulted in abnormal heart looping, although to a lesser extent. Combined KD of both Grk5 and Grk5l did not worsen the phenotype (Figures S1G and S1H). This implies that this function in early heart looping may be executed by both *grk5* genes.

From these data, we conclude that Grk5l influences development of the heart during its early formation.

Grk5l Governs Symmetry Breaking

Morphological defects of cardiac structures in the context of looping irregularities are indicators of disrupted LR asymmetry development. Similarly, human heterotaxy patients, who suffer from random placement of thoracic and/or abdominal organs, often develop dextrocardia as well as valvular or septal defects (i.e., common single ventricle). Thus, frequent complications in heterotaxy patients include CHDs. To test whether Grk5l might govern proper cardiogenesis by ensuring asymmetry development, we analyzed genes that are expressed unilaterally at specific developmental stages (Sutherland and Ware, 2009). Using whole-mount in situ hybridization (WMISH) at late somite stages (ss), we found that genes expressed in the left heart region, *bmp4* and the nodal target gene *lefty2*, are misexpressed upon Grk5l KD (Figures 2A and 2B). We then wondered whether Grk5l's impact on lateralization could be seen earlier on the level of the lateral plate mesoderm (LPM), which also gives rise to the heart. The LPM-specific genes *southpaw* (*spaw*) and *pitx2* were ambiguously expressed in Grk5l morphants (Figures 2C and 2D). However, this false pattern could be partially rescued by coinjection of MO-insensitive synthetic *grk5l* RNA (Figures 2C and 2D). Similarly, the correct distribution of *lefty2* could be rescued by *grk5l* RNA (Figure 2B). Analysis of *lefty1* expression in the left diencephalon, as well as pancreas placement in 2 days postfertilization (dpf) embryos further demonstrated that the lateralization defect upon loss of Grk5l is general (Figures 2E and 2F). Therefore, Grk5l may be an as yet unanticipated gene involved in the determination of LR asymmetry.

Cilia Length Depends on Grk5l

A prominent model in LR asymmetry development depends on the formation and function of cilia in the temporary organ of laterality (Kupffer's vesicle [KV] in zebrafish or the node in mice) (Sutherland and Ware, 2009). In line with this, zebrafish mutants for ciliary proteins often develop asymmetry defects, hydrocephalus, and a distinct body curvature (Sun et al., 2004). Such a

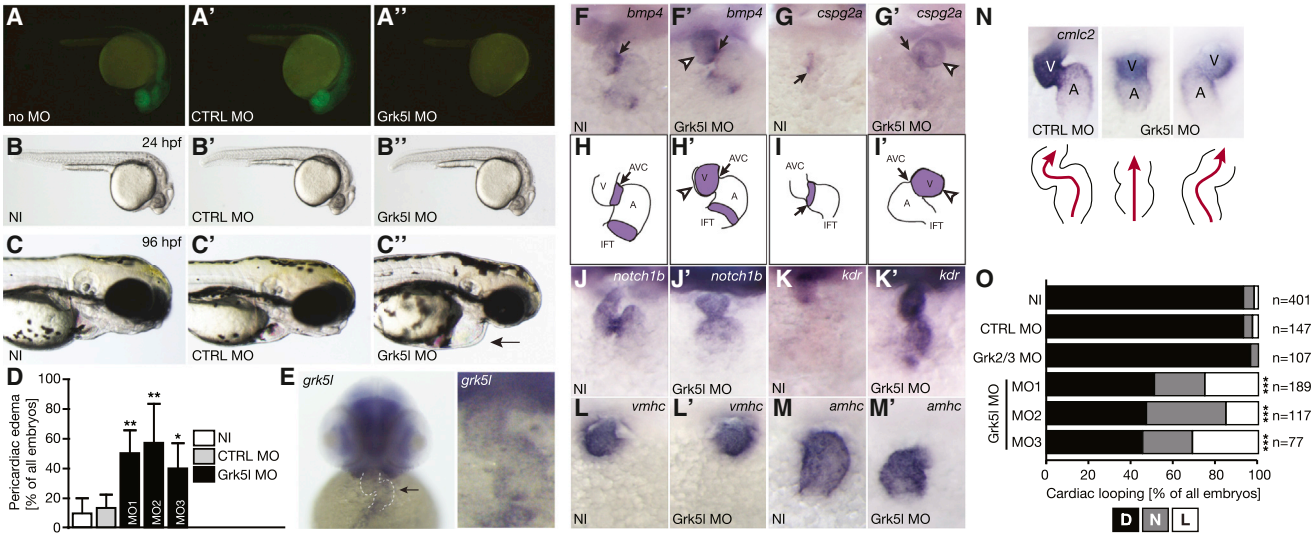

Figure 1. Grk5l KD in Zebrafish Affects Early Heart Development

(A–A″) Grk5l MO prevents translation of coinjected RNA coding for Grk5l-GFP fused to parts of its 5′ UTR and results in fish that show no glowing (A″), whereas RNA injection alone (A) or in combination with the CTRL MO (A′) produces strong GFP expression.

(B–B ″) Zebrafish embryos (24 hpf) injected with Grk5l MO (B″) compared with NI embryos (B) and embryos injected with CTRL MO (B′).

(C–C ″) Live embryos (96 hpf). Arrow indicates pericaridac edema in Grk5l morphants.

(D) Bar graph displaying the percentage of embryos with pericardiac edema as mean ± SEM. n = 3–10 experiments, 76–340 embryos. CTRL MO versus Grk5l MO: p = 0.0023; CTRL MO versus Grk5l MO2: p = 0.0016; CTRL MO versus Grk5l MO3: p = 0.0213.

(E) *grk5l* transcripts in the heart of 48 hpf zebrafish embryos (arrow and higher magnification).

(F and F') *bmp4* transcripts are upregulated and dispersed throughout the heart of Grk5l morphants (F'). n = 10–35.

(G and G′) Upregulation of *cspg2a* upon injection of Grk5l MO (G′). n = 16–18.

(H and H′) Illustration of normal distribution of *bmp4* in controls (H) and widespread expression in Grk5l morphants (H′).

(I and I′) Cartoon showing both regular and aberrant distribution of *cspg2a* in controls (I) and Grk5l MO (I') injected fish.

(J and J′) *Notch1b* fails to accumulate in the future valve region upon Grk5l KD (J′). n = 16–25.

(K and K′) *Kdr* is strongly upregulated upon KD of Grk5l (K′) compared with control fish (K). n = 5–22.

(L and L′) Ventricular fate as shown by WMISH for *vmhc* is properly established when Grk5l is lost. n = 27–32.

(M and M′) *Amhc* expression in the atrium. n = 18–23.

(N) WMISH for *cmlc2* at 50 hpf, revealing altered cardiac looping in Grk5l morphants (arrow). Cartoon depicts heart morphology and blood flow. A, atrium, V, ventricle.

(O) Summary of heart looping after injection with MOs targeting either Grk2/3 or Grk5l. For Grk5l, three different MOs were tested. D, D-loop, N, no loop, L, L-loop. CTRL MO versus Grk5l MO: $p < 0.0001$; CTRL MO versus Grk5l MO2: $p < 0.0001$; CTRL MO versus Grk5l MO3: $p < 0.0001$.

All images: 48–52 hpf (F–M). See also Figure S1 and Table S1.

curved body axis could also be observed upon depletion of Grk5l and was most prominent in embryos injected with MO3 (Figure S1F).

We thus questioned whether Grk5l might act on or within the KV, especially since we found transcripts of *grk5l*, which is expressed throughout development (Figures S2A–S2K), enriched in the tailbud region of embryos (Figures S2D–S2G).

First we tested whether the asymmetry defect was due to improper KV establishment. We analyzed midline formation as well as dorsal forerunner cell (DFC) clustering, both of which are essential processes preceding KV differentiation (Bisgrove et al., 1999; Oteíza et al., 2008). Neither of these processes was altered upon Grk5l KD (Figure 3A). Additionally, the KV area was not changed (Figures 3B and 3C), indicating that Grk5l may potentially exert its function within the KV itself.

To test this, we targeted the MO to DFCs, which are the cells that give rise to the KV. This can be achieved by injection at the 1k cell stage. MO or RNA is then specifically delivered to DFCs and thus the KV (Amack and Yost, 2004). This chimeric KD of Grk5l was sufficient to interfere with proper heart looping as well as pancreas placement (Figures 3D and 3E). In addition, we observed randomization of *spaw* expression (Figure 3F). We next wondered if Grk5l would localize to cilia. We detected Grk5l in primary cilia when expressed in NIH 3T3 cells and in motile cilia in the pronephric duct (Figure 3G). We therefore investigated whether Grk5l KD would affect cilia formation in zebrafish. Motile cilia of the developing pronephros were longer in Grk5l morphants compared with control embryos (Figures 3H and 3I). These results suggested that a ciliary defect in the KV may be the basis for the Grk5l phenotype. Although we did not observe a significant change in cilia number (Figures 3J and 3K), we found that the cilia of Grk5l-depleted KVs were significantly longer than those in control injected embryos (Figures 3J and 3L). These findings are again in line with the common observation that zebrafish with ciliary deficiencies display a pronounced body curvature, which we also observed (Figure S1F). These results suggest that Grk5l helps to regulate cilia formation in the developing embryo, thereby ensuring symmetry breaking.

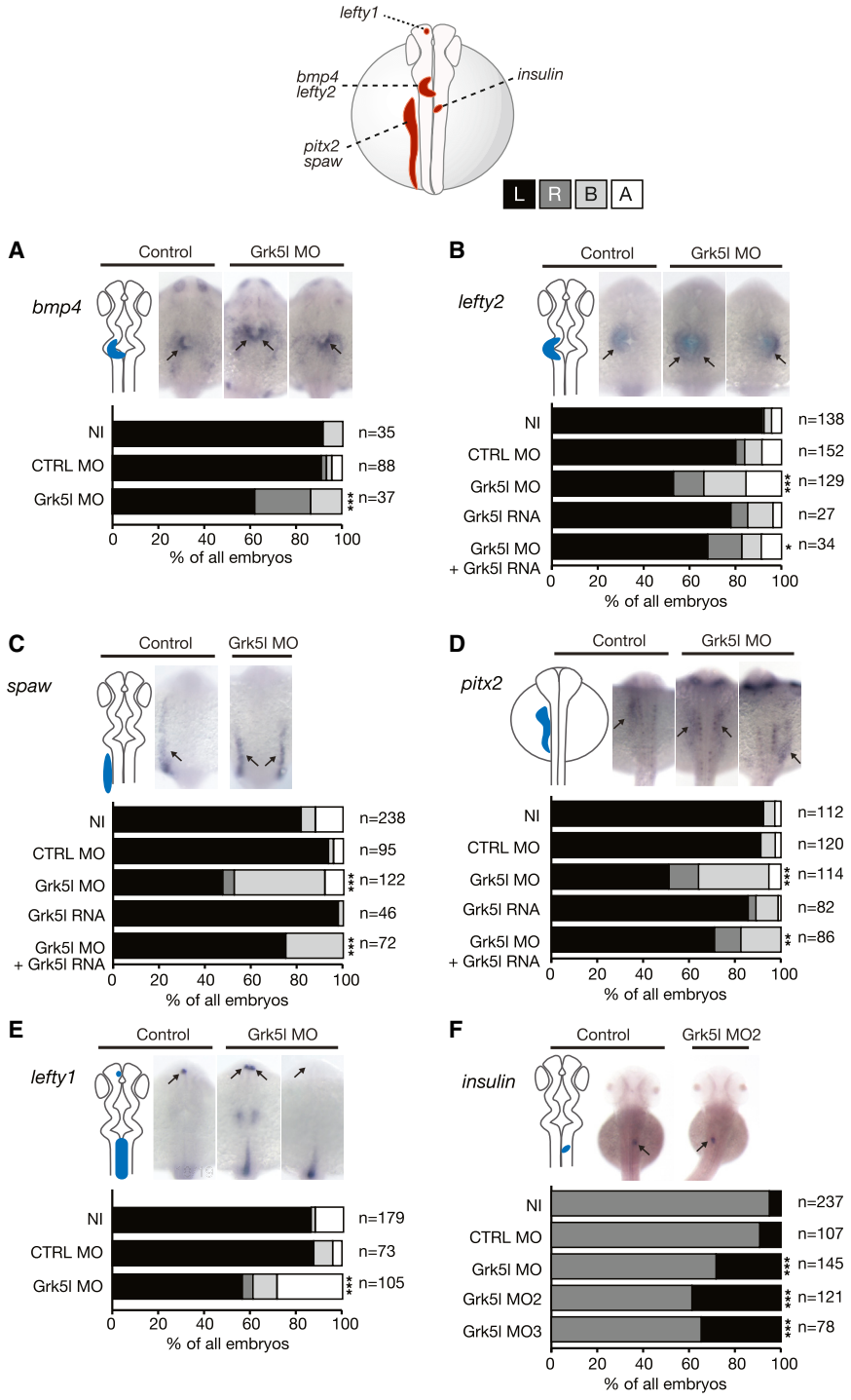

Figure 2. Grk5l Governs LR Asymmetry Development

WMISH for leftward marker genes at 20–22 ss with the respective expression domain outlined next to the images. Bar graphs display percentages of expression on the left side (black), the right side (dark gray), and both sides of the midline (light gray), or no expression at all (white).

(A) *bmp4* expression in the heart region is randomized upon Grk5l KD. CTRL MO versus Grk5l MO: $p = 0.0056$.

(B) Random distribution of *lefty2* can be partially rescued by *grk5l* RNA. CTRL MO versus Grk5l MO: $p < 0.0001$; Grk5l MO versus Grk5l MO+*grk5l* RNA: $p = 0.0425$.

(C) *spaw* in the LPM is affected upon loss of Grk5l, but can be rescued by coinjection of *grk5l* mRNA. CTRL MO versus Grk5l MO: $p < 0.0001$; Grk5l MO versus Grk5l MO+*grk5l* RNA: $p = 0.0002$.

(D) Ambiguous *pitx2* reversed by mRNA encoding for *grk5l*. CTRL MO versus Grk5l MO: $p < 0.0001$; Grk5l MO versus Grk5l MO+*grk5l* RNA: $p = 0.0068$.

(E) *Lefty1* transcripts in the dorsal diencephalon are ambiguously distributed when Grk5l is lost. CTRL MO versus Grk5l MO: $p < 0.0001$.

(F) Loss of Grk5l interferes with pancreas placement, as can be seen by the expression of *insulin*. CTRL MO versus Grk5l MO: $p = 0.0009$; CTRL MO versus Grk5l MO2: $p < 0.0001$; CTRL MO versus Grk5l MO3: $p < 0.0001$.

Grk5l Fine-Tunes mTOR Complex 1 Activity during Symmetry Breaking

We next wanted to identify the molecular mechanism that causes the Grk5l KD phenotype. Overstimulation of α_{1b}-adrenoceptors (α_{1b}-AR) can cause lateralization defects (Fujinaga et al., 1994). Because GRK5 attenuates elevated α_{1b}-AR signaling (Eckhart et al., 2000), we hypothesized that the observed phenotype could be caused by loss of Grk5l-mediated α_{1b}-AR desensitization. However, WD-4101, an α_{1b}-AR-specific inhibitor, did not rescue situs inversus frequency in Grk5l KD embryos (Figure S3A). We thus wondered if the observed phenotype could potentially be due to Grk5l modulating signaling not at the level of GPCRs. However, we found no differences when we studied target gene expression of the Shh or retinoic acid signaling in Grk5l morphants (Figures S3B–S3D″). Both pathways were previously implicated in symmetry breaking (Huang et al., 2011a; Schilling et al., 1999).

We previously reported that Grk5 facilitates canonical Wnt signaling (Chen et al., 2009). Because Grk5l might share this function, we tested its effect on *axin2* (Figure S3E). Grk5l appears to be a positive modulator of canonical Wnt signaling. Canonical Wnt signaling has also been reported to steer LR asymmetry development (Caron et al., 2012). However, impaired Wnt signaling is associated with shorter cilia, whereas we see elongated cilia. Therefore, Grk5l's action on Wnt signaling may not necessarily be related to its role in asymmetry development.

Recent studies of ciliary diseases, including PKD and heterotaxy, have highlighted the importance of mTOR complex 1

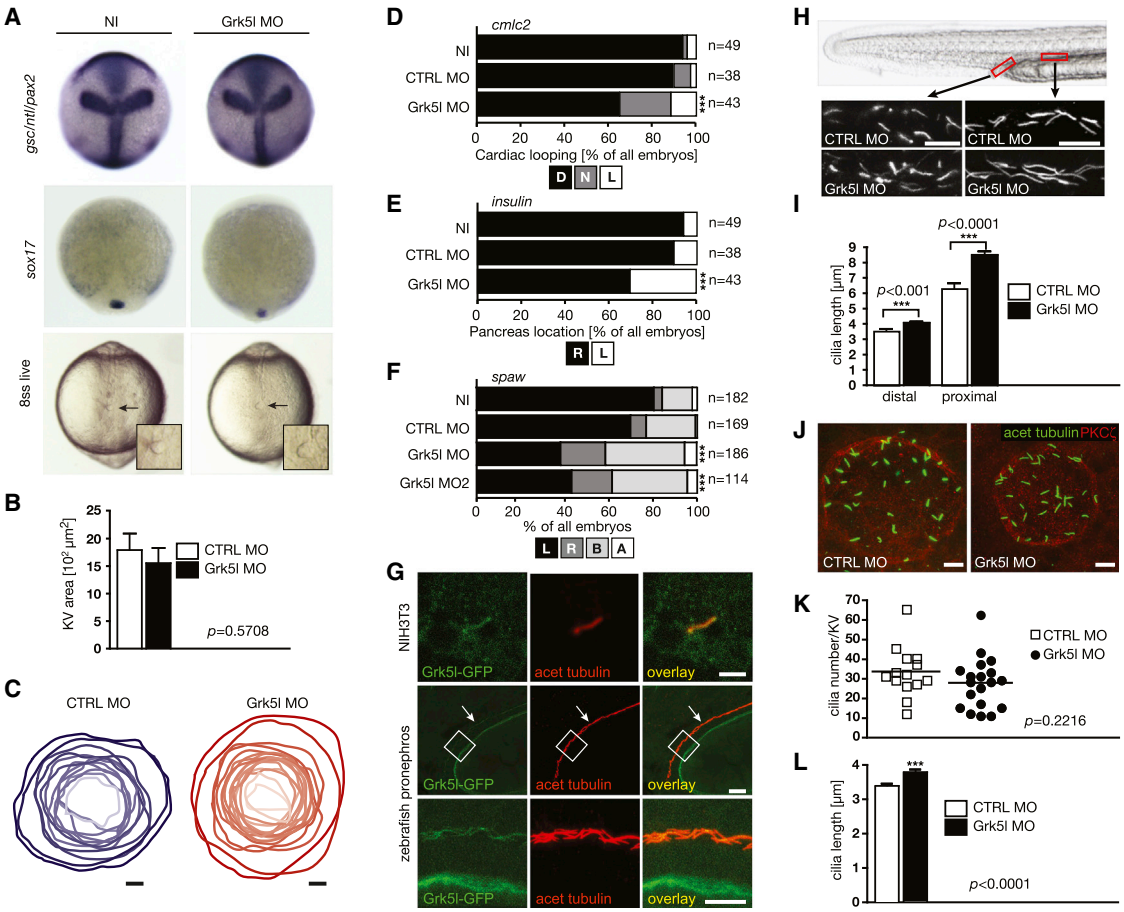

Figure 3. Grk5l Acts in the Organ of Laterality

(A) Combined WMISH for *gsc*, *ntl*, and *pax2* (10 hpf). DFCs cluster normally at 90% epiboly as shown by *sox17* (n = 32–35). Live imaging at 8 ss shows that the KV forms. Arrows indicate KV; higher magnification in inset.

(B) KV-specific KD did not alter KV area as assessed by PKCζ staining at 8 ss. n = 14–19 embryos. CTRL MO: 1,793 ± 299 µm^2, Grk5l MO: 1,555 ± 277 µm^2. Bar graph displays means ± SEM.

(C) Outline of KVs upon injection of CTRL MO (blue) or Grk5l MO (red). Depending on the respective size, the KV is shown in darker or brighter shading. n = 12–17 embryos.

(D) Impaired heart looping by Grk5l depletion in KV cells detected by *cmlc2* ISH at 50 hpf. CTRL MO versus Grk5l MO: p < 0.0001.

(E) *insulin*-positive cells of the pancreas are more often on the left side of the midline upon KV-specific KD of Grk5l. CTRL MO versus Grk5l MO: p = 0.0007.

(F) KV-directed ablation of Grk5l randomizes *spaw*. CTRL MO versus Grk5l MO: p < 0.0001; CTRL MO versus Grk5l MO2: p = 0.0002.

(G) Grk5l localizes to primary cilia in NIH 3T3 cells and motile cilia in the developing zebrafish kidney. Images show Grk5l-GFP after transfection in cells or injection of capped RNA into one-cell-stage embryos. Scale bars, 3 µm (NIH 3T3), 20 µm (low magnification of pronephros), and 10 µm (higher magnification).

(H) Elongation of motile cilia of the zebrafish pronephros (2 dpf). Cilia in the distal (CTRL MO: 3.571 ± 0.116 µm, Grk5l MO: 4.090 ± 0.0852 µm) and proximal part (CTRL MO: 6.347 ± 0.318 µm, Grk5l MO: 8.526 ± 0.220 µm) were analyzed. Approximate areas of analysis are indicated in red in the live image of a 2 dpf zebrafish tail. Scale bar, 10 µm.

(I) Bar graph summarizing pronephric cilia measurements as means ± SEM (n = 32–101 cilia).

(J) Motile cilia at 8 ss with MOs targeted to KV cells. Images were selected for cilia length. Scale bar, 10 µm.

(K) Cilia number was not altered in the KV by MOs targeted to the KV (8 ss). n = 14–19 embryos. CTRL MO: 34.14 ± 3.372 cilia; Grk5l MO: 28.53 ± 2.960 cilia.

(L) Grk5l depletion in the KV increases cilia length. n = 460–513 cilia at 8 ss. CTRL MO: 3.344 ± 0.049 µm; Grk5l MO: 3.748 ± 0.054 µm; p < 0.0001, two-tailed, unpaired t test. Bar graph displays means ± SEM.

See also Figure S2.

(mTORC1), which regulates cell growth (Zoncu et al., 2011). mTORC1 signaling has been connected to ciliary architecture and function, and thus conditions that rely on cilia (Boehlke et al., 2010; DiBella et al., 2009; Yuan et al., 2012). We therefore investigated whether Grk5l influences mTORC1 activity by measuring phosphorylation of its target S6K1 in zebrafish embryos. We detected an increase in mTORC1 activity, indicating a negative impact of Grk5l on mTORC1 activity (Figure 4A). This finding was reproduced in the hearts of young GRK5 knockout (KO) mice (Figure 4B). In addition, we found that transient overexpression of Grk5l in human embryonic kidney 293T (HEK293T) cells caused a reduction of mTORC1 activity

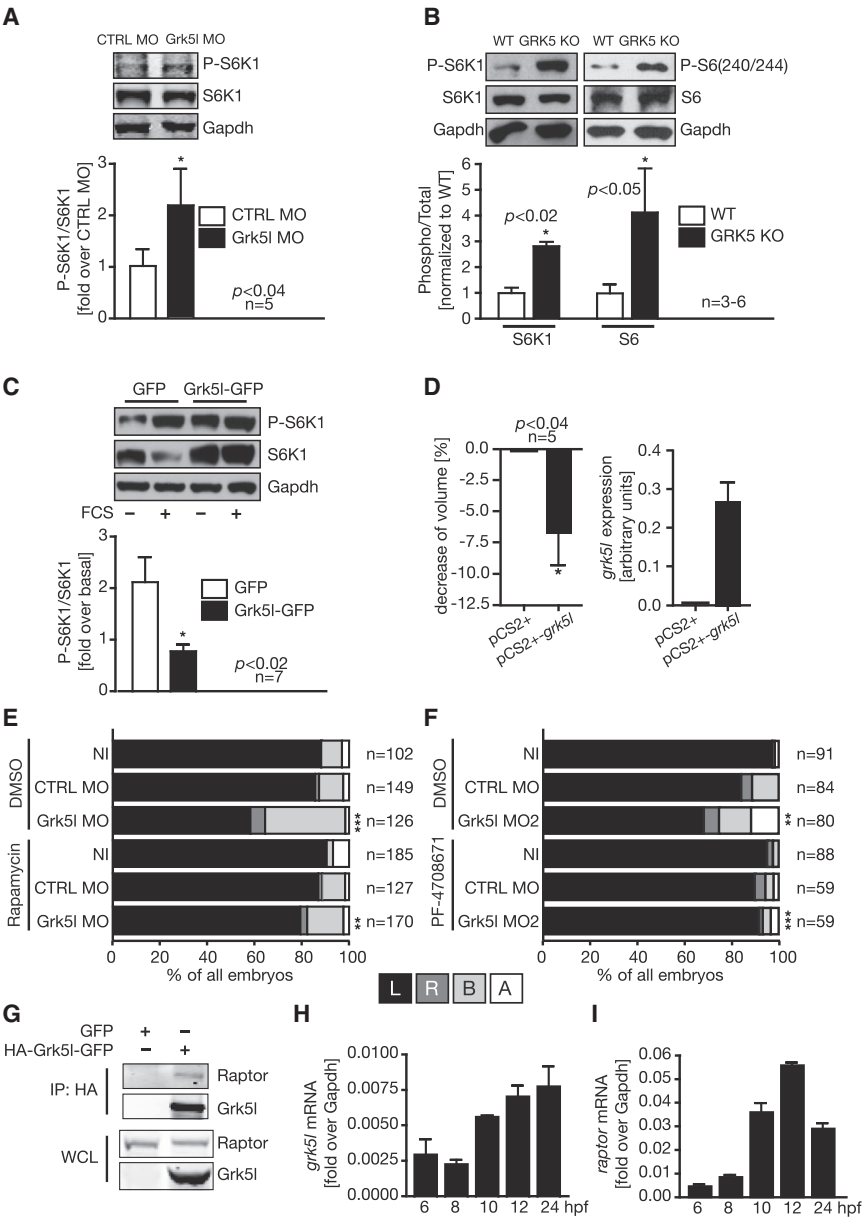

Figure 4. Grk5l Limits mTOR Signaling

(A) Western blot analysis of zebrafish embryos (6–8 ss) for S6K1 phosphorylation. Representative images of a single blot are shown. Bar graph displays means ± SEM.

(B) Western blot of mouse heart lysates of WT and GRK5 KO mice for phosphorylation of S6K1 and its target ribosomal protein S6. Bar graph displays means ± SEM.

(C) Overexpression of Grk5l-GFP in cells attenuates TORC1 activity toward S6K1. Bar graph displays means ± SEM.

(D) Cell volume of Grk5l transfected cells (left: mean ± SEM). Cells were controlled for *grk5l* expression (right graph: means ± SD, n = 2–3).

(E) Reversal of the Grk5l lateralization phenotype by rapa. Analysis of *spaw* in the presence of DMSO or rapa from 6 to 10 hpf. CTRL MO^{DMSO} versus Grk5l MO^{DMSO}: $p < 0.0001$; Grk5l MO^{DMSO} versus Grk5l MO^{Rapa}: $p = 0.0033$.

(F) Inhibition of S6K1 activity by PF-470871 reverses *spaw* misexpression upon Grk5l KD. CTRL MO^{DMSO} versus Grk5l $MO2^{DMSO}$: $p = 0.0063$; Grk5l $MO2^{DMSO}$ versus Grk5l $MO2^{PF}$: $p < 0.0001$.

(G) Coimmunoprecipitation of transfected GFP or hemagglutinin (HA)-Grk5l-GFP and endogenous Raptor using an HA antibody. IP, immunoprecipitation; WCL, whole-cell lysate.

(H) Relative expression levels of *grk5l* obtained by qPCR (mean ± SD, n = 2).

(I) *raptor* mRNA levels (mean ± SD, n = 2).

See also Figures S2, S3, and S4.

(Figure 4C) and a decrease in cell volume (Figure 4D). These results suggest that depletion of Grk5l might remove a dampening effect on mTORC1 activity and that an apparent mTORC1 overstimulation would be causal for the lateralization defect. To test this, we treated Grk5l KD embryos with the mTORC1 inhibitor rapamycin (rapa). Rapa rescued the lateralization phenotype of Grk5l KD embryos (Figures 4E and S4A), whereas control embryos were unaffected. Furthermore, a specific S6K1 inhibitor (Pearce et al., 2010; Rosner et al., 2012) could also rescue the phenotype (Figure 4F). We conclude from this that increased mTORC1 activity is causal for the asymmetry defects in the Grk5l KD embryos. To determine whether there may be a direct physical interaction, we performed coimmunoprecipitation assays in transfected as well as native cells. Raptor coprecipitated with overexpressed Grk5l (Figure 4G) as well as endogenous GRK5 (Figure S4B). Grk5l also colocalized with the mTORC1 components mTOR, Raptor, and mLST8 in HEK293T cells (data not shown). These data are in line with our in vivo results and corroborate the finding that Grk5l negatively regulates mTORC1 activity, probably through direct interaction with Raptor.

We also analyzed the spatial expression patterns of *grk5l* and *raptor* and found them to be very similar (Figure S2). Moreover, the mRNA levels of both *grk5l* and *raptor* substantially increase at 10 hpf (Figures 4H and 4I), when the KV (the essential structure for symmetry breaking) starts to form. We thus reasoned that a rescue of the Grk5l KD phenotype might also be achieved by inhibition of mTORC1 from 10 hpf on, which is what we observed (Figure S4A). Moreover, randomization of laterality could also be reversed by rapa when Grk5l was knocked down specifically in the KV (Figure S4C). We conclude that Grk5l is needed to fine-tune mTORC1 activity at the level of the temporal organ of laterality in order to accomplish successful symmetry breaking.

Previously, it has always been assumed that GRK5 would be dispensable for embryonic development, primarily because GRK5 KO mice are viable (Gainetdinov et al., 1999). Yet, the

combined loss of GRK5 and GRK6 results in embryonic lethality (Table S1). A detailed characterization of this lethality remains to be undertaken and will be the subject of future studies in our lab.

In this study, we used zebrafish to delineate the importance of vertebrate GRK5 during development. Similar to GRK5 KO mice, depletion of Grk5l in zebrafish does not necessarily result in embryonic lethality, but in a complex, often overlooked embryonic phenotype. Similarly, heterotaxy can have a number of mild phenotypes that are easily missed. Future studies will thus be required to illuminate whether and how GRK5 influences symmetry breaking in mammals.

In summary, we have provided evidence that vertebrate GRK5 possesses physiological relevance during development of the heart. We found that the close homolog in zebrafish, Grk5l, is required to steer lateralization in zebrafish. In this way, it ensures proper cardiogenesis and may potentially prevent CHDs, which are common complications in situs anomalies. Mechanistically, Grk5l confines mTORC1 signaling at the level of the temporal organ of asymmetry and controls ciliary morphology. Moreover, Grk5l potentially influences heart morphology by affecting the expression of cardiac genes. The well-characterized role that vertebrate GRK5 plays in the adult heart thus needs to be expanded to very early steps during development, when the body plan and thus a properly functioning heart are defined.

EXPERIMENTAL PROCEDURES

Zebrafish and Mouse Experiments

Zebrafish were maintained in standard conditions under a 14-hr-light and 10-hr-dark cycle. Fertilized eggs were injected and allowed to develop at 28.5°C. Mice lacking GRK5 and/or GRK6 were generated as described previously (Gainetdinov et al., 1999, 2003) and bred from heterozygous breeding pairs. Tissue for western blotting was harvested from 3- to 5-month-old animals. The mice were housed under a 12-hr-light/dark cycle in an SPF facility. All husbandry and experiments described here were approved by German authorities or by the IACUC at Duke University.

For further details regarding the materials and methods used, please refer to the Extended Experimental Procedures.

SUPPLEMENTAL INFORMATION

Supplemental Information includes Extended Experimental Procedures, four figures, and one table and can be found with this article online at http://dx.doi.org/10.1016/j.celrep.2013.07.036.

ACKNOWLEDGMENTS

We thank the Zebrafish International Resource Center and many colleagues for providing reagents, Sabrina Matysik for technical assistance, Cornelia Donow for help with the MO binding assay, and Jim Burris and Julia Schäfer for fish maintenance. This work was supported in part by FP7 of the European Commission (M.P.), Deutsche Stiftung für Herzforschung (M.P.), and NIH grants NS-019576 and MH-073853 (M.G.C.). During the initial stages of this work, M.P. was the recipient of a Marie Curie Outgoing International Fellowship from the European Commission.

Received: November 17, 2012
Revised: June 27, 2013
Accepted: July 25, 2013
Published: August 22, 2013

REFERENCES

Amack, J.D., and Yost, H.J. (2004). The T box transcription factor no tail in ciliated cells controls zebrafish left-right asymmetry. Curr. Biol. *14*, 685–690.

Bisgrove, B.W., Essner, J.J., and Yost, H.J. (1999). Regulation of midline development by antagonism of lefty and nodal signaling. Development *126*, 3253–3262.

Boehlke, C., Kotsis, F., Patel, V., Braeg, S., Voelker, H., Bredt, S., Beyer, T., Janusch, H., Hamann, C., Gödel, M., et al. (2010). Primary cilia regulate mTORC1 activity and cell size through Lkb1. Nat. Cell Biol. *12*, 1115–1122.

Caron, A., Xu, X., and Lin, X. (2012). Wnt/β-catenin signaling directly regulates Foxj1 expression and ciliogenesis in zebrafish Kupffer's vesicle. Development *139*, 514–524.

Chen, E.P., Bittner, H.B., Akhter, S.A., Koch, W.J., and Davis, R.D. (2001). Myocardial function in hearts with transgenic overexpression of the G protein-coupled receptor kinase 5. Ann. Thorac. Surg. *71*, 1320–1324.

Chen, M., Philipp, M., Wang, J., Premont, R.T., Garrison, T.R., Caron, M.G., Lefkowitz, R.J., and Chen, W. (2009). G Protein-coupled receptor kinases phosphorylate LRP6 in the Wnt pathway. J. Biol. Chem. *284*, 35040–35048.

DiBella, L.M., Park, A., and Sun, Z. (2009). Zebrafish Tsc1 reveals functional interactions between the cilium and the TOR pathway. Hum. Mol. Genet. *18*, 595–606.

Eckhart, A.D., Duncan, S.J., Penn, R.B., Benovic, J.L., Lefkowitz, R.J., and Koch, W.J. (2000). Hybrid transgenic mice reveal in vivo specificity of G protein-coupled receptor kinases in the heart. Circ. Res. *86*, 43–50.

Essner, J.J., Vogan, K.J., Wagner, M.K., Tabin, C.J., Yost, H.J., and Brueckner, M. (2002). Conserved function for embryonic nodal cilia. Nature *418*, 37–38.

Fujinaga, M., Hoffman, B.B., and Baden, J.M. (1994). Receptor subtype and intracellular signal transduction pathway associated with situs inversus induced by alpha 1 adrenergic stimulation in rat embryos. Dev. Biol. *162*, 558–567.

Gainetdinov, R.R., Bohn, L.M., Walker, J.K., Laporte, S.A., Macrae, A.D., Caron, M.G., Lefkowitz, R.J., and Premont, R.T. (1999). Muscarinic supersensitivity and impaired receptor desensitization in G protein-coupled receptor kinase 5-deficient mice. Neuron *24*, 1029–1036.

Gainetdinov, R.R., Bohn, L.M., Sotnikova, T.D., Cyr, M., Laakso, A., Macrae, A.D., Torres, G.E., Kim, K.M., Lefkowitz, R.J., Caron, M.G., and Premont, R.T. (2003). Dopaminergic supersensitivity in G protein-coupled receptor kinase 6-deficient mice. Neuron *38*, 291–303.

Gold, J.I., Gao, E., Shang, X., Premont, R.T., and Koch, W.J. (2012). Determining the absolute requirement of G protein-coupled receptor kinase 5 for pathological cardiac hypertrophy: short communication. Circ. Res. *111*, 1048–1053.

Huang, S., Ma, J., Liu, X., Zhang, Y., and Luo, L. (2011a). Retinoic acid signaling sequentially controls visceral and heart laterality in zebrafish. J. Biol. Chem. *286*, 28533–28543.

Huang, Z.M., Gold, J.I., and Koch, W.J. (2011b). G protein-coupled receptor kinases in normal and failing myocardium. Front. Biosci. *17*, 3047–3060.

Jaffe, K.M., Thiberge, S.Y., Bisher, M.E., and Burdine, R.D. (2010). Imaging cilia in zebrafish. Methods Cell Biol. *97*, 415–435.

Liggett, S.B., Cresci, S., Kelly, R.J., Syed, F.M., Matkovich, S.J., Hahn, H.S., Diwan, A., Martini, J.S., Sparks, L., Parekh, R.R., et al. (2008). A GRK5 polymorphism that inhibits beta-adrenergic receptor signaling is protective in heart failure. Nat. Med. *14*, 510–517.

Martini, J.S., Raake, P., Vinge, L.E., DeGeorge, B.R., Jr., Chuprun, J.K., Harris, D.M., Gao, E., Eckhart, A.D., Pitcher, J.A., and Koch, W.J. (2008). Uncovering G protein-coupled receptor kinase-5 as a histone deacetylase kinase in the nucleus of cardiomyocytes. Proc. Natl. Acad. Sci. USA *105*, 12457–12462.

Michal, A.M., So, C.H., Beeharry, N., Shankar, H., Mashayekhi, R., Yen, T.J., and Benovic, J.L. (2012). G Protein-coupled receptor kinase 5 is localized to centrosomes and regulates cell cycle progression. J. Biol. Chem. *287*, 6928–6940.

Okada, Y., Takeda, S., Tanaka, Y., Izpisúa Belmonte, J.C., and Hirokawa, N. (2005). Mechanism of nodal flow: a conserved symmetry breaking event in left-right axis determination. Cell *121*, 633–644.

Oteíza, P., Köppen, M., Concha, M.L., and Heisenberg, C.P. (2008). Origin and shaping of the laterality organ in zebrafish. Development *135*, 2807–2813.

Pearce, L.R., Alton, G.R., Richter, D.T., Kath, J.C., Lingardo, L., Chapman, J., Hwang, C., and Alessi, D.R. (2010). Characterization of PF-4708671, a novel and highly specific inhibitor of p70 ribosomal S6 kinase (S6K1). Biochem. J. *431*, 245–255.

Philipp, M., Fralish, G.B., Meloni, A.R., Chen, W., MacInnes, A.W., Barak, L.S., and Caron, M.G. (2008). Smoothened signaling in vertebrates is facilitated by a G protein-coupled receptor kinase. Mol. Biol. Cell *19*, 5478–5489.

Pierpont, M.E., Basson, C.T., Benson, D.W., Jr., Gelb, B.D., Giglia, T.M., Goldmuntz, E., McGee, G., Sable, C.A., Srivastava, D., and Webb, C.L.; American Heart Association Congenital Cardiac Defects Committee, Council on Cardiovascular Disease in the Young. (2007). Genetic basis for congenital heart defects: current knowledge: a scientific statement from the American Heart Association Congenital Cardiac Defects Committee, Council on Cardiovascular Disease in the Young: endorsed by the American Academy of Pediatrics. Circulation *115*, 3015–3038.

Premont, R.T., and Gainetdinov, R.R. (2007). Physiological roles of G protein-coupled receptor kinases and arrestins. Annu. Rev. Physiol. *69*, 511–534.

Premont, R.T., Macrae, A.D., Aparicio, S.A., Kendall, H.E., Welch, J.E., and Lefkowitz, R.J. (1999). The GRK4 subfamily of G protein-coupled receptor kinases. Alternative splicing, gene organization, and sequence conservation. J. Biol. Chem. *274*, 29381–29389.

Ramsdell, A.F. (2005). Left-right asymmetry and congenital cardiac defects: getting to the heart of the matter in vertebrate left-right axis determination. Dev. Biol. *288*, 1–20.

Rockman, H.A., Choi, D.J., Rahman, N.U., Akhter, S.A., Lefkowitz, R.J., and Koch, W.J. (1996). Receptor-specific in vivo desensitization by the G protein-coupled receptor kinase-5 in transgenic mice. Proc. Natl. Acad. Sci. USA *93*, 9954–9959.

Rosner, M., Schipany, K., and Hengstschläger, M. (2012). p70 S6K1 nuclear localization depends on its mTOR-mediated phosphorylation at T389, but not on its kinase activity towards S6. Amino Acids *42*, 2251–2256.

Schilling, T.F., Concordet, J.P., and Ingham, P.W. (1999). Regulation of left-right asymmetries in the zebrafish by Shh and BMP4. Dev. Biol. *210*, 277–287.

Sorriento, D., Santulli, G., Fusco, A., Anastasio, A., Trimarco, B., and Iaccarino, G. (2010). Intracardiac injection of AdGRK5-NT reduces left ventricular hypertrophy by inhibiting NF-kappaB-dependent hypertrophic gene expression. Hypertension *56*, 696–704.

Sun, Z., Amsterdam, A., Pazour, G.J., Cole, D.G., Miller, M.S., and Hopkins, N. (2004). A genetic screen in zebrafish identifies cilia genes as a principal cause of cystic kidney. Development *131*, 4085–4093.

Sutherland, M.J., and Ware, S.M. (2009). Disorders of left-right asymmetry: heterotaxy and situs inversus. Am. J. Med. Genet. C. Semin. Med. Genet. *151C*, 307–317.

Yuan, S., Li, J., Diener, D.R., Choma, M.A., Rosenbaum, J.L., and Sun, Z. (2012). Target-of-rapamycin complex 1 (Torc1) signaling modulates cilia size and function through protein synthesis regulation. Proc. Natl. Acad. Sci. USA *109*, 2021–2026.

Zoncu, R., Efeyan, A., and Sabatini, D.M. (2011). mTOR: from growth signal integration to cancer, diabetes and ageing. Nat. Rev. Mol. Cell Biol. *12*, 21–35.

Zullo, A., Iaconis, D., Barra, A., Cantone, A., Messaddeq, N., Capasso, G., Dollé, P., Igarashi, P., and Franco, B. (2010). Kidney-specific inactivation of Ofd1 leads to renal cystic disease associated with upregulation of the mTOR pathway. Hum. Mol. Genet. *19*, 2792–2803.